Ocean Engineering 199 (2020) 106820

Contents lists available at ScienceDirect

Ocean Engineering

journal homepage: www.elsevier.com/locate/oceaneng

Robust dynamic positioning of autonomous surface vessels with tube-based model predictive control

Huarong Zheng [a], Jun Wu [a], Weimin Wu [a,*], Yifeng Zhang [b]

[a] The State Key Laboratory of Industrial Control Technology, College of Control Science and Engineering, Zhejiang University, Hangzhou, China
[b] Binhai Industrial Technology Research Institute of Zhejiang University, Tianjin, China

ARTICLE INFO

Keywords:
Robust dynamic positioning
Model predictive control
Output feedback control
Observer
Autonomous surface vessels

ABSTRACT

This paper proposes two robust dynamic positioning (DP) approaches for autonomous surface vessels when full states are measurable and when only partial states are available with measurement errors. High fidelity nonlinear hydrodynamics are considered which are approximated as linear models in the local area of DP setpoint. The linearization errors are seen as bounded unmodeled dynamics and are accommodated in the tube-based model predictive control (MPC) together with environmental disturbances. The tube-based MPC controller contains all the possible uncertain trajectories in a tube that is based on a precomputed robust positive invariant set and a nominal trajectory solved online. The total controller consists of a feedforward part compensating the predicted environmental forces, a nominal part guiding the vessel towards and stabilizing it at the origin, and an affine feedback part bounding the uncertain vessel trajectory within the tube. Furthermore, an output feedback robust DP controller is proposed by utilizing a simple Luenberger observer to estimate the system states when full states are not available. The resultant estimation and measurement errors are also incorporated in the tube-based MPC. Simulation results show that the proposed full state and output feedback robust DP controllers can achieve the DP goals within system constraints.

1. Introduction

Autonomous surfaces vessels (ASVs) have been widely used for various purposes, e.g., military, environment monitoring and rescue (Zheng et al., 2013). ASVs can be seen as a special type of robotic systems in the sense that they can comprehend the surroundings and figure out what to do autonomously. However, the major difference of ASVs with the frequently encountered ground robots is that ASVs maneuver in the fluid. Therefore, usually complex hydrodynamics are involved and the system itself cannot stay at its equilibrium when exposed to the fluid disturbances. Besides, sensors for localization and velocities are generally more expensive with degraded performance over water. These issues brought about new challenges in maintaining ASVs in a fixed position for offshore operations.

Principally, there are two ways to maintain a fixed ASV pose over water by using external mooring lines/tethers or by thrusters. The case when thrusters are exclusively used is the so-called dynamic positioning (DP) and is known to be more flexible (Fossen, 2011). The large body of literature on DP control systems until 2011 are reviewed and discussed in (Sørensen, 2011) and the references therein. Representative DP control methods include the widely implemented PID controllers (Cetin and Akkaya, 2010), nonlinear passivity theory based control (Fossen and Strand, 1999), and sliding mode control (Tannuri et al., 2010). The methods in (Fossen and Strand, 1999) (Tannuri et al., 2010) can deal with vessel nonlinear hydrodynamics directly while PID usually needs to be equipped with gain scheduling (Torsetnes et al., 2004) or fuzzy logic (Cetin and Akkaya, 2010) designs to deal with nonlinearities. However, these methods are often associated with tedious tuning procedure, and the control performance differs when the environment, load or tasks change. The environmental disturbances also play an important role in the DP control performance. Kalman filter or the extended Kalman filter (Fossen and Perez, 2009) (Sørensen et al., 1996) is commonly used for estimating the vessel motion states and for filtering disturbances working together with the previous mentioned controllers. However, most Kalman filter based designs assume that the "separation" principle holds so that the controller and the observer could be designed separately, which is not valid if system constraints are imposed.

More recent approaches utilize integrated controller and observer designs and achieve robust bounded control performance when uncertain environmental disturbances exist. An adaptive backstepping control

* Corresponding author.
E-mail address: wmwu@iipc.zju.edu.cn (W. Wu).

https://doi.org/10.1016/j.oceaneng.2019.106820
Received 15 August 2019; Received in revised form 3 December 2019; Accepted 3 December 2019
Available online 6 February 2020

law is proposed in (Witkowska and Śmierzchalski, 2018) to accommodate the unknown environmental disturbances. System constraints are considered in the low-level control allocation problem. The high-gain observer approach with an auxiliary dynamic system to deal with the estimation error has been popular in DP control systems, see, e.g., (Du et al., 2015) (Du et al., 2016) (Lin et al., 2018). In (Du et al., 2015), the robustness against unknown system dynamic parameters, unmeasured velocities and unknown time-varying disturbances is achieved by combining adaptive neural networks and high-gain observer into the backstepping method. The not considered input saturation in (Du et al., 2015) is treated in (Du et al., 2016). A similar high-gain observer approach using an adaptive fuzzy system to approximate any continuous system with arbitrary small error is proposed in (Lin et al., 2018) for DP. Four observer and integral action based methods for compensating of bias loads in DP of vessels are compared in (Værnø et al., 2019). The bias loads estimated from the designed observers with fine tuning can generally work well for the DP problem. Note that all these controller derivations are based on linear hydrodynamic drag in vessel dynamics. However, the real vessel dynamics are inherently nonlinear, and the effects of the unmodeled dynamics in the presence of environmental disturbances should be kept in mind. Besides, the DP task is often accomplished without considering the control efforts taken, i.e., not in an optimal way. By employing the vessel parallel coordinate and linear hydrodynamic drag (Fossen, 2011), linear control methods such as linear quadratic Gaussian (Fossen and Perez, 2009) (Sørensen et al., 1996) can be applied to achieve optimal control performance. However, using a new coordinate system might complicate the problem formulation if design criteria or system limitations are specified in the conventional coordinate system. Moreover, since optimal solutions generally occur on the boundary of feasible regions, the unmodeled dynamics, as uncertainties, could degrade the control performance or result in actuator failures if not properly handled.

In addition to systematically handling system constraints and optimizing performance, model predictive control (MPC) (Mayne, 2014), can be designed to be robust to various types of disturbances, e.g., unmodeled dynamics (Yan and Wang, 2012), bounded (Mayne et al., 2005) and stochastic disturbances (Kouvaritakis et al., 2010). In robust MPC, an intuitive idea is to compute the open-loop predicted trajectory by taking into account of all possible realizations of uncertainties over the prediction horizon. Min-max routines can then be applied as in (Yan and Wang, 2012) (Jia and Krogh, 2002). However, this could lead to conservativeness and even infeasibility. Incorporating feedback in predictions have, therefore, become standard practice for controlling uncertain systems using MPC. Tube-based MPC which has the same order of complexity as that of conventional MPC trades-off complication and conservativeness with an affine local feedback policy (Mayne et al., 2005). The tube containing all possible system trajectories uses a nominal trajectory as its center and uncertainties that are steered to the center by the local feedback as cross sections. Rigorous robust MPC synthesis has been derived for a class of constrained linear discrete-time invariant system with bounded disturbances (Mayne et al., 2005), (Raković et al., 2012). Robust MPC has been successfully applied to the stabilization (Li and Yan, 2017), tracking (Zheng et al., 2016a), integrated motion and torque allocation (Veksler et al., 2016), distributed tracking control (Zheng et al., 2018) and vessel platooning (Chen et al., 2018) problems of marine surface vessels. System robustness against uncertainties, optimal control performance and constraint satisfactions are systematically achieved when all the states can be measured accurately. However, localization and velocity states of marine surface vessels are usually only measured partially with errors. Moreover, due to the complexity of the utilized prediction models, closed-loop system properties are not analyzed (Zheng et al., 2018). Research on DP of ASVs with system constraints, unmodeled system dynamics, partially measured states with errors and uncertain environmental disturbances using MPC, to the best of our knowledge, has not been presented in the literature to date.

In this paper, we propose using tube-based MPC to design robust DP controllers for ASVs in dealing with all these factors simultaneously. In face of system constraints, nonlinear hydrodynamics, partially measured system states with errors and uncertain external environmental forces, the vessel can still converge to and maintain within a bounded neighborhood of the specified DP pose at optimal control efforts. For the convenience of controller design and tractability of the MPC optimization problems, we approximate the system dynamics in the local area of DP as a linear uncertain model by Jacobian linearization at the equilibrium point. The unmodeled dynamics act as a type of additional bounded disturbances in addition to the environmental uncertainties. Both full state feedback and output feedback robust DP controllers are designed in the framework of tube-based MPC. A Luenberger observer is designed to estimate the system states when only partially inaccurate states are available. Simulation results demonstrate the effectiveness of the proposed robust DP controllers.

The remainder of the paper is organized as follows. Section 2 presents the DP problem formulation and the dynamic models of ASVs. Then in Section 3, the robust DP controller with tube-based MPC is first proposed when full system states are available. When system states are only measured partially, an output feedback robust MPC controller is further proposed in Section 4. Section 5 presents simulation results and discussions, followed by concluding remarks and future research directions in Section 6.

2. Modeling of ASVs for DP

For designing the DP robust controller that maintains the vessel's position and heading, we consider the three degree-of-freedom (DOF) low-frequency marine surface vessel motion model on the horizontal plane, as shown in Fig. 1. The vessel's motions are influenced not only by active thrusters, but also by the uncontrollable environmental disturbances due to wind, waves, and currents in open waters. Dynamics of surface vessels considering forces and moment due to wind, waves and currents are modeled following the notations in (Fossen, 2011) as:

$$\dot{\boldsymbol{\eta}}(t) = \boldsymbol{R}(\psi(t))\boldsymbol{\nu}(t), \tag{1}$$

$$\begin{aligned}\dot{\boldsymbol{\nu}}(t) = \boldsymbol{M}^{-1}\big(\boldsymbol{\tau}(t) + \bar{\boldsymbol{\tau}}_{\text{env}}(t) + \boldsymbol{b}(t) - \\ \boldsymbol{C}(\boldsymbol{\nu}(t))\boldsymbol{\nu}(t) - \boldsymbol{D}(\boldsymbol{\nu}(t))\boldsymbol{\nu}(t)\big)\end{aligned} \tag{2}$$

where $\boldsymbol{R}(\psi(t))$ is the rotation matrix converting motions from body-fixed frame $\{b\}$ to the inertial north-east-down frame $\{n\}$ with

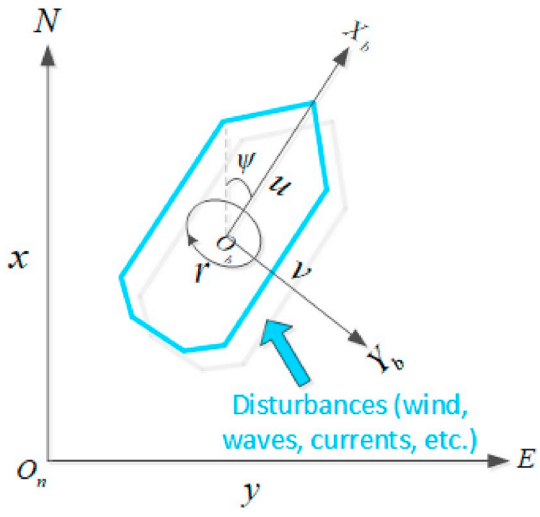

Fig. 1. Motions of waterborne AGV system in $\{n\}$ and $\{b\}$ with environmental disturbances.

$$\boldsymbol{R}(\psi(t)) = \begin{bmatrix} \cos(\psi(t)) & -\sin(\psi(t)) & 0 \\ \sin(\psi(t)) & \cos(\psi(t)) & 0 \\ 0 & 0 & 1 \end{bmatrix}.$$

$\boldsymbol{M} \in \mathbb{R}^{3\times3}$ is the mass matrix including the rigid-body mass and added mass. $\boldsymbol{C}(\boldsymbol{\nu}(t)) \in \mathbb{R}^{3\times3}$ is the nonlinear coriolis and centripetal matrix, and $\boldsymbol{D}(\boldsymbol{\nu}(t)) \in \mathbb{R}^{3\times3}$ is the nonlinear damping matrix.

System states $[\boldsymbol{\eta}^{\mathrm{T}}(t), \boldsymbol{\nu}^{\mathrm{T}}(t)]^{\mathrm{T}} = [x(t), y(t), \psi(t), u(t), v(t), r(t)]^{\mathrm{T}}$ are translational/rotational positions and speeds in $\{n\}$ and $\{b\}$, respectively. The control input force is $\boldsymbol{\tau}(t) = [\tau_u(t), \tau_v(t), \tau_r(t)]^{\mathrm{T}}$ from the active thrusters on surge, sway and yaw. Generally, marine surface vessels only set schedules to travel in a certain limit of weather conditions based on weather forecast. For example, the port authority cooperates with local water management organizations and installs hydrological and meteorological sensors at different locations in the Port of Rotterdam to provide information ranging from visibility, tides, flow rates, wave heights to wind speeds and directions (Port of Rotterdam, 2015). However, predictions with weather forecast and sensor information are not accurate enough and are usually with prediction errors. Therefore, we assume that the uncontrollable predicted input $\overline{\boldsymbol{\tau}}_{\mathrm{env}}(t)$ due to environmental disturbances could in principle be obtained from the meteorological predictions, but with bounded uncertain prediction errors $\boldsymbol{b}(t) \in \mathbb{W}$ with $\mathbb{W}$ being a compact set containing the origin in the interior, and $\overline{\boldsymbol{\tau}}_{\mathrm{env}}(t) = [\overline{\tau}_{u,\mathrm{env}}(t), \overline{\tau}_{v,\mathrm{env}}(t), \overline{\tau}_{r,\mathrm{env}}]^{\mathrm{T}}$, $\boldsymbol{b}(t) = [b_u(t), b_v(t), b_r(t)]^{\mathrm{T}}$. When those extreme disturbances do occur or when the weather forecast accuracy cannot be guaranteed, rarely though, extra safety and recovery mechanisms need to be designed, which falls out of the scope of this paper.

The certain limit of weather condition a surface vessel can be against to is limited by the designed thrust and power capacity. Therefore, the physical limitations on vessel motions and inputs need to be satisfied as:

$$\boldsymbol{\eta}_{\min} \leq \boldsymbol{\eta}(t), \leq \boldsymbol{\eta}_{\max}, \tag{3}$$

$$\boldsymbol{\nu}_{\min} \leq \boldsymbol{\nu}(t) \leq \boldsymbol{\nu}_{\max}, \tag{4}$$

$$\boldsymbol{\tau}_{\min} \leq \boldsymbol{\tau}(t) \leq \boldsymbol{\tau}_{\max}, \tag{5}$$

where $\bullet_{\min}$ and $\bullet_{\max}$ denote minimal and maximal values of corresponding parameters.

For scenarios over water, sensors like GPS and accelerometer are usually installed on marine structure to measure the system states. However, high accuracy sensors are usually expensive and speed sensors are frequently not installed. Denote the measured system output $\boldsymbol{y}(t)$ as

$$\boldsymbol{y}(t) = \boldsymbol{C}\left[\boldsymbol{\eta}^{\mathrm{T}}(t), \boldsymbol{\nu}^{\mathrm{T}}(t)\right]^{\mathrm{T}} + \boldsymbol{v}. \tag{6}$$

Based on (6), when all the system states $[\boldsymbol{\eta}^{\mathrm{T}}(t), \boldsymbol{\nu}^{\mathrm{T}}(t)]^{\mathrm{T}}$ can be measured accurately, $\boldsymbol{C} = \boldsymbol{I}_{6\times6}$ and $\boldsymbol{v} = 0$, a full state feedback robust controller is designed in Section 3. When only localization sensors are available and measurement errors exist, i.e., $\boldsymbol{C} = [\boldsymbol{I}_{3\times3}, 0_{3\times3}]$ and $\boldsymbol{v} \neq 0$, an output feedback robust controller is designed in Section 4.

3. Robust DP control with full state feedback

In this section, considering the nonlinear uncertain vessel dynamics (1)–(2) with full state feedback, we design a robust DP controller with tube-based MPC (Mayne et al., 2005). The vessel is guaranteed to converge to and maintain at a bounded neighborhood of the specified DP position and heading with as small as possible control efforts. All state and actuator constraints are satisfied in spite of environmental disturbances. Specifically, a feedforward controller is first designed converting the equilibrium point of (1)–(2) to the origin. Then, linearization at the equilibrium point of the feedforward controlled system is applied to decompose the system into a linear time invariant model and higher-order Taylor series terms. The higher-order terms together with the environmental uncertainties are treated as bounded errors which are then accommodated in the designed tube-based MPC controller.

3.1. Feedforward control and linearization

Given the predicted environmental force values $\overline{\boldsymbol{\tau}}_{\mathrm{env}}(t)$, define

$$\boldsymbol{u}(t) = \boldsymbol{\tau}(t) + \overline{\boldsymbol{\tau}}_{\mathrm{env}}(t), \tag{7}$$

i.e., the actually implemented thruster forces are $\boldsymbol{\tau}(t) = \boldsymbol{u}(t) - \overline{\boldsymbol{\tau}}_{\mathrm{env}}(t)$ with feedforward compensation for the predicted environmental forces. Then, the vessel dynamics (1)–(2) is generalized for notational consistency and simplicity as:

$$\dot{\boldsymbol{x}} = f(\boldsymbol{x}(t), \boldsymbol{u}(t), \boldsymbol{b}(t)) \tag{8}$$

with $f : \mathbb{R}^6 \times \mathbb{R}^3 \times \mathbb{R}^3 \to \mathbb{R}^6$ being continuous and $f(0,0,0) = 0$. System states, control inputs and unknown disturbance inputs are represented by $\boldsymbol{x}(k) \in \mathbb{R}^6$, $\boldsymbol{u}(k) \in \mathbb{R}^3$ and $\boldsymbol{b}(k) \in \mathbb{R}^3$, respectively. The nonlinearity and uncertainty in (8) with constraints (3)–(5) render a robust controller design and implementation extremely difficult if not impossible. Therefore, for computational efficiency and controller design easiness, we apply Jacobian linearizations to (8) at the origin and approximate (8) as:

$$\dot{\boldsymbol{x}} = \boldsymbol{A}_c\boldsymbol{x}(t) + \boldsymbol{B}_c\boldsymbol{u}(t) + \boldsymbol{E}_c\boldsymbol{b}(t) + \varepsilon(t) \tag{9}$$

where

$$\boldsymbol{A}_c = \frac{\partial f}{\partial \boldsymbol{x}}|_{(0,0,0)}, \boldsymbol{B}_c = \frac{\partial f}{\partial \boldsymbol{u}}|_{(0,0,0)}, \boldsymbol{E}_c = \frac{\partial f}{\partial \boldsymbol{b}}|_{(0,0,0)},$$

and $\varepsilon(t) \in \mathbb{R}^6$ represents the higher-order Taylor series term. Since f is continuous, $\boldsymbol{x}, \boldsymbol{u}, \boldsymbol{b}$ are all bounded and contains the origin in the interior, the linearization error $\varepsilon(t) \in \mathbb{E}$ which is also bounded and contains the origin in its interior, and $\varepsilon(t) = 0$ when $(\boldsymbol{x}, \boldsymbol{u}, \boldsymbol{b}) = (0,0,0)$. Note that linearized vessel dynamics have also been successfully applied in tracking controller designs in (Zheng et al., 2016b) (Zheng et al., 2014). The performance of using the original nonlinear dynamics (1)–(2) and linearized prediction models of marine surface vessels in MPC has been compared in (Zheng et al., 2014). The performance of the linearized MPC without considering the effects of linearization errors is comparable to the nonlinear MPC. By treating the linearization errors as bounded uncertainties that are then handled in the tube-based control framework is, therefore, expected to achieve better performance. For numerical simulations, (9) is usually discretized by zero-order-hold assumption as:

$$\boldsymbol{x}(k+1) = \boldsymbol{A}\boldsymbol{x}(k) + \boldsymbol{B}\boldsymbol{u}(k) + \boldsymbol{E}\boldsymbol{b}(k) + \varepsilon(k) \tag{10}$$

where $\boldsymbol{A}$, $\boldsymbol{B}$ and $\boldsymbol{E}$ are the discrete time matrices corresponding to $\boldsymbol{A}_c$, $\boldsymbol{B}_c$ and $\boldsymbol{E}_c$. Moreover, for the considered vessel dynamics, $(\boldsymbol{A}, \boldsymbol{B})$ is controllable and $(\boldsymbol{A}, \boldsymbol{C})$ is observable. The discrete time k relates to t as $t = kT_s$ with sampling time T_s.

3.2. Robust DP with tube-based MPC

For the DP problem of ASVs, the main idea of tube-based robust MPC (Mayne et al., 2005) is to contain all the possible uncertain vessel trajectories in a tube. The tube center is generated by solving online nominal convex optimization problems and the tube cross section is precomputed offline as robust positive invariant sets based on (10) and the bounded uncertainties. Controlled vessel trajectories for every possible realization of the uncertainties then evolve around the tube center within the tube and converge to the specified DP position and heading.

For the MPC problem, we consider the predicted vessel trajectories over a future finite prediction horizon N_{p} (Zheng et al., 2016b). Whenever contextually clear, we denote $(i|k)$ as the ith prediction step at time step k with $i = 0, 1, \ldots, N_{\mathrm{p}} - 1$ for control inputs and $i = 0, 1, \ldots, N_{\mathrm{p}}$

for system states. Then, the uncertain predicted system state trajectories $\boldsymbol{x}(i|k)$ are partitioned as

$$\boldsymbol{x}(i|k) = \bar{\boldsymbol{x}}(i|k) + \boldsymbol{e}(i|k), \tag{11}$$

where $\bar{\boldsymbol{x}}$ denotes the nominal state trajectory, and $\boldsymbol{e}$ is the deviation of the actual state $\boldsymbol{x}(i|k)$ from the nominal state $\bar{\boldsymbol{x}}(i|k)$. On the one hand, the tube cross section may be unnecessarily large resulting in conservativeness if an open-loop control sequence without feedback is directly employed. On the other hand, optimizing over arbitral feedback policies is untractable. Therefore, the simple affine feedback policy is introduced to restrict the size of tube cross sections as

$$\boldsymbol{u}(i|k) = \bar{\boldsymbol{u}}(i|k) + \boldsymbol{K}\boldsymbol{e}(i|k) \tag{12}$$

where $\boldsymbol{K}$ is a time-invariant feedback gain and is chosen such that $\boldsymbol{A}_{\boldsymbol{K}} = \boldsymbol{A} + \boldsymbol{B}\boldsymbol{K}$ is stable. In our case, $\boldsymbol{K}$ is computed offline as the feedback gain of the infinite-horizon linear quadratic regulator for the unconstrained system (10) with proper weighting matrices. Then, we could decompose the closed-loop system with (12) as a nominal part

$$\bar{\boldsymbol{x}}(i+1|k) = \boldsymbol{A}\bar{\boldsymbol{x}}(i|k) + \boldsymbol{B}\bar{\boldsymbol{u}}(i|k) \tag{13}$$

and an uncertain part

$$\boldsymbol{e}(i+1|k) = \boldsymbol{A}_{\boldsymbol{K}}\boldsymbol{e}(i|k) + \boldsymbol{E}\boldsymbol{b}(i|k) + \varepsilon(i|k) \tag{14}$$

where $\boldsymbol{b} \in \mathbb{W}$ and $\varepsilon \in \mathbb{E}$. Denote the sets for the uncertain system dynamics (14) as $\mathbb{S}(i)$, i.e., $\boldsymbol{e}(i|k) \in \mathbb{S}(i)$, we further have:

$$\mathbb{S}(i+1) := \boldsymbol{A}_{\boldsymbol{K}}\mathbb{S}(i) \oplus \boldsymbol{E}\mathbb{W} \oplus \mathbb{E},$$

and therefore,

$$\mathbb{S}(i) = \boldsymbol{A}_{\boldsymbol{K}}^{i}\mathbb{S}(0) + \sum_{j=0}^{i-1} \boldsymbol{A}_{\boldsymbol{K}}^{j}(\boldsymbol{E}\mathbb{W} \oplus \mathbb{E}). \tag{15}$$

Note that since the system matrices of (10) and the compact sets $\mathbb{W}$, $\mathbb{E}$ are all time-invariant, the set $\mathbb{S}(i)$ is also irrelevant with time step k. Moreover, the sets $\{\mathbb{S}(i)\}$ are expected to be smaller than those calculated from open-loop unstable $\boldsymbol{A}$ since $\boldsymbol{A}_{\boldsymbol{K}}$ is now stable by design. The operator $\oplus$ denotes the Minkowski set sum defined as $A \oplus B := \{a+b|a \in A, b \in B\}$ with some abuse of notations.

Since $\boldsymbol{A}_{\boldsymbol{K}}$ is stable, the robust positive invariant set $\mathbb{S}(\infty)$ exists for (15) (Mayne et al., 2005), i.e., $\forall i, \forall \boldsymbol{b} \in \mathbb{W}, \forall \varepsilon \in \mathbb{E}$, if $\boldsymbol{e}(0|k) \in \mathbb{S}(\infty)$, then $\boldsymbol{e}(i|k) \in \mathbb{S}(\infty), \forall i \in \boldsymbol{I}_{i>0}$. However, the computation of $\mathbb{S}(\infty)$ is difficult. In practice, we could compute an robust positive invariant outer approximation set $\mathbb{S} \supseteq \mathbb{S}(\infty)$ as in (Rakovic et al., 2005) with $\mathbb{S} = (1-\alpha)^{-1}\mathbb{S}(N_p)$. To reduce conservativeness, $\alpha \in (0,1)$ should be chosen suitably small.

Therefore, (11) can be written as a tube $\{\mathbb{X}(i|k)\}$ with $\{\bar{\boldsymbol{x}}(i|k)\}$ as the center and $\{\mathbb{S}\}$ as cross sections, as demonstrated in Fig. 2, would be:

$$\mathbb{X}(i|k) := \bar{\boldsymbol{x}}(i|k) \oplus \mathbb{S}. \tag{16}$$

Likewise, (12) is written as

$$\mathbb{U}(i|k) := \bar{\boldsymbol{u}}(i|k) \oplus \boldsymbol{K}\mathbb{S}. \tag{17}$$

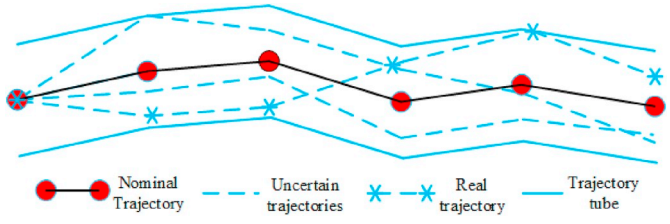

Fig. 2. Trajectory tube with nominal trajectory as the center and bounded uncertain trajectories as cross sections.

If $\mathbb{C}_x$ and $\mathbb{C}_u$ are denoted as system state and input constraint sets, respectively, imposed by actual system constraints (3)–(5), and $\mathbb{C}_{x_f}$ is denoted as the terminal positive invariant constraint set (Mayne et al., 2000) for (10) with $\mathbb{C}_x$ and $\mathbb{C}_u$, then all state and input trajectories by tubes (16)–(17) need to satisfy:

$$\mathbb{X}(i|k) \subseteq \mathbb{C}_x,\ \mathbb{X}(N_p|k) \subseteq \mathbb{C}_{x_f},\ \mathbb{U}(i|k) \subseteq \mathbb{C}_u$$

Equivalently, the nominal state and input trajectories $\bar{\boldsymbol{x}}(i|k)$ and $\bar{\boldsymbol{u}}(i|k)$ need to satisfy tighter constraints as:

$$\bar{\boldsymbol{x}}(i|k) \subseteq \mathbb{C}_x \ominus \mathbb{S}, \tag{18}$$

$$\bar{\boldsymbol{x}}(N_p|k) \subseteq \mathbb{C}_{x_f} \ominus \mathbb{S}, \tag{19}$$

$$\bar{\boldsymbol{u}}(i|k) \subseteq \mathbb{C}_u \ominus \boldsymbol{K}\mathbb{S} \tag{20}$$

where the operator $\ominus$ denotes Minkowski set difference defined as $A \ominus B := \{a - b|a \in A, b \in B\}$.

Assumption 1. *The bounded uncertainties* $\mathbf{b}$ *and* $\boldsymbol{\varepsilon}$ *are all small so that* $\mathbb{S} \in \mathbb{C}_x$, $\mathbb{S} \in \mathbb{C}_{x_f}$ *and* $K\mathbb{S} \in \mathbb{C}_u$.

Assumption 1 can be satisfied if the vessel only operates when the weather forecast is precise and operates within a local area of the DP setpoint. Large system constraint sets could also help tolerate relatively large uncertainty values. With Assumption 1, the nominal optimal predictive control problem for the robust DP of ASVs is then readily formulated as:

$$\min_{\bar{\boldsymbol{u}}(i|k)} \left|\left|\bar{\boldsymbol{x}}(N_p|k)\right|\right|_{\boldsymbol{Q}_f}^2 + \sum_{i=0}^{N_p-1} \left|\left|\bar{\boldsymbol{x}}(i|k)\right|\right|_{\boldsymbol{Q}}^2 + \left|\left|\bar{\boldsymbol{u}}(i|k)\right|\right|_{\boldsymbol{R}}^2 \tag{21}$$

subject to (13), (18)–(20).

The nominal cost function (21) aims to steer the nominal state trajectory to the origin with optimal control efforts. The three terms are the terminal cost, the stage cost, and the control input cost. The notation $\left|\left|\bar{\boldsymbol{x}}(i|k)\right|\right|_{\boldsymbol{Q}}^2 = \bar{\boldsymbol{x}}(i|k)^{\mathrm{T}}\boldsymbol{Q}\bar{\boldsymbol{x}}(i|k)$, and the same go for the control input cost and the terminal cost. $\boldsymbol{Q}$, $\boldsymbol{Q}$ and $\boldsymbol{Q}_f$ are positive definite weighting matrices for the respective cost terms and can be adjusted to set priority between convergence speed and control efforts. The terminal weight matrix $\boldsymbol{Q}_f$ is chosen as the solution to the corresponding Riccati equation (Mayne, 2014). The robust positive invariant set $\mathbb{S}$, feedback gain $\boldsymbol{K}$, terminal weighting matrix $\boldsymbol{Q}_f$, and the terminal constraint set $\mathbb{C}_{x_f}$ can all be precomputed offline. The online optimization problem (21) subject to (13), (18)–(20) has comparable computational complexity with that of the conventional MPC. Moreover, with Assumption 1, the nominal problem is feasible and is guaranteed to converge to the system origin (Mayne et al., 2000). Then, the uncertain system is guaranteed to converge to a bounded neighborhood $\mathbb{S}$ around the origin.

4. Output feedback robust controller design

In the previous section, we have considered the robust DP problem using tube-based MPC with full state feedback, i.e., $\boldsymbol{C} = \boldsymbol{I}_{6\times6}$ and $\boldsymbol{v} = 0$. However, system states are usually only partially and roughly available over water due to the cost and inaccuracy of marine application oriented sensors. Therefore, we extend the full state feedback robust DP controller to an output feedback robust controller (Mayne et al., 2006) in this section. A Luenberger observer is designed to estimate the system states based on the output. Measurement errors and estimation errors are both accommodated by treating them as extra system bounded disturbances.

We now consider only the vessel pose states are available, i.e., $\boldsymbol{C} = [\boldsymbol{I}_{3\times3}, 0_{3\times3}]$ and there exist unknown bounded measurement errors, i.e., $\boldsymbol{v} \in \mathbb{V}$ with $\mathbb{V}$ being a compact set containing the origin in its interior. With output $\boldsymbol{y}$, we design the Luenberger observer dynamics as

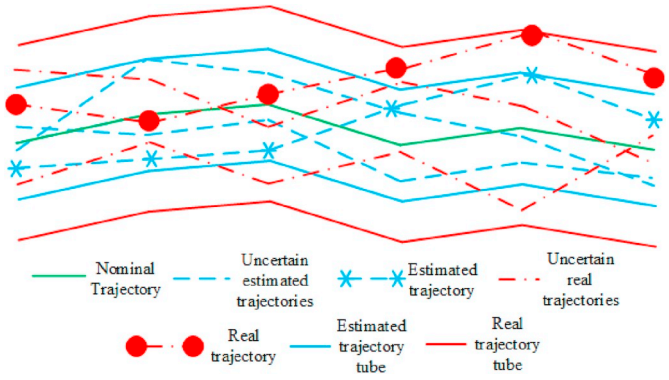

Fig. 3. Trajectory tube with output feedback.

$$\hat{\boldsymbol{x}}(k+1) = \boldsymbol{A}\hat{\boldsymbol{x}}(k) + \boldsymbol{B}\boldsymbol{u}(k) + \boldsymbol{L}(\boldsymbol{y}(k) - \hat{\boldsymbol{y}}(k)), \tag{22}$$

$$\hat{\boldsymbol{y}}(k) = \boldsymbol{C}\hat{\boldsymbol{x}}(\boldsymbol{k}) \tag{23}$$

where $\hat{\boldsymbol{x}}(k) \in \mathbb{R}^6$ is the estimated state at time step k and $\boldsymbol{L}$ is Luenberger observer gain with $\boldsymbol{L}^{\mathrm{T}} = \boldsymbol{G}\boldsymbol{X}^{-1}$ where $\boldsymbol{G}$ is a arbitrary matrix set to the identity matrix hereby, and $\boldsymbol{X}$ is the solution to the Sylvester equation (Hou et al., 1999):

$$\boldsymbol{A}^{\mathrm{T}}\boldsymbol{X} - \boldsymbol{X}\boldsymbol{A}_K = \boldsymbol{C}^{\mathrm{T}}\boldsymbol{G}.$$

Combining (10), (6), (22) and (23), we have

$$\tilde{\boldsymbol{x}}(k+1) = \boldsymbol{A}_L\tilde{\boldsymbol{x}}(k) + (\boldsymbol{E}\boldsymbol{b}(k) + \varepsilon(k) - \boldsymbol{L}\boldsymbol{v}) \tag{24}$$

where $\tilde{\boldsymbol{x}}(k) = \boldsymbol{x}(k) - \hat{\boldsymbol{x}}(k)$ is the state estimation error and $\boldsymbol{A}_L = \boldsymbol{A} - \boldsymbol{L}\boldsymbol{C}$ with $\rho(\boldsymbol{A}_L) < 1$ by design. The estimation error of (22) from (9) can be bounded as a robust positive invariant set as in (15). Since $\rho(\boldsymbol{A}_L) < 1$, $(\boldsymbol{E}\boldsymbol{b}(k) + \varepsilon(k) - \boldsymbol{L}\boldsymbol{v})$ is a compact set containing the origin in its interior, there exists a robust positive invariant set $\tilde{\mathbb{S}}$ so that if $\tilde{\boldsymbol{x}}(k) \in \tilde{\mathbb{S}}$, then $\forall\, \boldsymbol{b}(k) \in \mathbb{W}, \forall \varepsilon \in \mathbb{E}, \forall \boldsymbol{v} \in \mathbb{V}$, $\tilde{\boldsymbol{x}}(k+1) \in \tilde{\mathbb{S}}$. To extend the tube-based MPC design in Section 3, we can now consider (13) as the nominal observer dynamics for (22) instead of the state dynamics (9), and bound the real state trajectory $\boldsymbol{x}(k)$ around $\hat{\boldsymbol{x}}(k)$.

With some abuse of notations, define $\boldsymbol{e}(k) = \hat{\boldsymbol{x}}(k) - \bar{\boldsymbol{x}}(k)$ now as the error between the observer state and nominal state, the affine feedback policy $\boldsymbol{u}(k) = \bar{\boldsymbol{u}}(k) + \boldsymbol{K}\boldsymbol{e}(k)$ then the closed-loop observer dynamics are

$$\hat{\boldsymbol{x}}(k+1) = \boldsymbol{A}\hat{\boldsymbol{x}}(k) + \boldsymbol{B}\bar{\boldsymbol{u}}(k) + \boldsymbol{B}\boldsymbol{K}\boldsymbol{e}(k) + \boldsymbol{L}(\boldsymbol{C}\tilde{\boldsymbol{x}}(k) + \boldsymbol{v}(k)), \tag{25}$$

with $\tilde{\boldsymbol{x}}(k) \in \tilde{\mathbb{S}}$. Combining (13) with (25), (14) becomes

$$\boldsymbol{e}(i+1|k) = \boldsymbol{A}_K\boldsymbol{e}(i|k) + \boldsymbol{L}(\boldsymbol{C}\tilde{\boldsymbol{x}}(k) + \boldsymbol{v}(k)), \tag{26}$$

and $\boldsymbol{A}_K$ is the same as before and is stable by design. Since $\boldsymbol{L}(\boldsymbol{C}\tilde{\boldsymbol{x}}(k) + \boldsymbol{v}(k))$ is compact and contains the origin in its interior, there still exists the robust positive invariant set $\mathbb{S}$ for (26). Therefore, we now can confine the real state trajectory which is

$$\boldsymbol{x}(k) = \bar{\boldsymbol{x}}(k) + \tilde{\boldsymbol{x}}(k) + \boldsymbol{e}(k) \tag{27}$$

in a tube with $\bar{\boldsymbol{x}}(k)$ as the center and $\mathbb{S} + \tilde{\mathbb{S}}$ as the cross section, as shown in Fig. 3. The nominal state and input trajectory can be obtained by solving a similar problem with (21). The overall robust DP with output feedback tube-based MPC can be implemented as Algorithm 1. Note Step 4 is implemented in case the bounded disturbance assumptions are not satisfied.

Algorithm 1. Output feedback robust DP for ASVs.

1: Initialize at $k = 0$, set $\bar{\boldsymbol{x}}(0) = \boldsymbol{x}(0)$, $\hat{\boldsymbol{x}}(0) = \boldsymbol{x}(0)$; linearize (8) to obtain the linear prediction model; compute sets $\mathbb{S}$, $\tilde{\mathbb{S}}$, $\mathbb{C}_{x_f}$, terminal weighting matrix $\boldsymbol{Q}_f$;
2: **while** kT_s is smaller than the set simulation time **do**
3: Solve the nominal optimization problem (21) subject to (13), (18) – (20), and obtain the nominal control input sequence $\bar{\boldsymbol{u}}(i|k)$;
4: Check: if $\hat{\boldsymbol{x}}(k) \notin \bar{\boldsymbol{x}}(k) \oplus \mathbb{S} \oplus \tilde{\mathbb{S}}$, then set $\bar{\boldsymbol{x}}(0|k) = \hat{\boldsymbol{x}}(k)$ and resolve the nominal optimization problem;
5: Apply $\boldsymbol{u}(k) = \bar{\boldsymbol{u}}(0|k) + \boldsymbol{K}(\hat{\boldsymbol{x}}(k) - \bar{\boldsymbol{x}}(k)) - \bar{\boldsymbol{\tau}}_{\mathrm{env}}(k)$ to the real system (1) – (2);
6: Compute the successor observer state $\hat{\boldsymbol{x}}(k+1)$ by (22) and the nominal state $\bar{\boldsymbol{x}}(k+1)$ by (13);
7: Set $k = k+1$, $\hat{\boldsymbol{x}}(0|k) = \hat{\boldsymbol{x}}(k)$, $\bar{\boldsymbol{x}}(0|k) = \bar{\boldsymbol{x}}(k)$ and go to Step 3;
8: **end while**

5. Simulation results and discussions

Simulations are carried out to demonstrate the effectiveness of the proposed robust DP algorithms for ASVs with full state feedback and output feedback. The vessel is initially positioned at a location away from the origin and is controlled to converge to and maintain at the origin with specified heading in spite of environmental disturbances due to wind, waves, and currents. It is assumed that the environmental forces acting on the vessel hull can be predicted. However, there exist bounded prediction errors. In the simulations, the considered uncertainties $\boldsymbol{b}$, ε and $\boldsymbol{v}$ are implemented as random but bounded values, i.e., numbers that follow normal distribution but are truncated with lower/upper bounds. In (Fossen and Strand, 1999) (Fossen and Perez, 2009), uncertainties are also considered as white Gaussian noises following normal distributions. Particularly, the boundary values for the uncertainties are set as: $||\boldsymbol{b}|| \leq 0.28$, $\varepsilon \leq 0.2$, and $||\boldsymbol{v}|| \leq 0.2$. Controller parameters are set as follows: prediction horizons $N_{\mathrm{p}} = 6$ for the full state feedback controller and $N_{\mathrm{p}} = 10$ for the output feedback controller; weight parameter $\boldsymbol{Q} = diag([10\ 10\ 0.1\ 0.1\ 0.1\ 0.1])$ where *diag* means diagonal matrices, $\boldsymbol{R} = \boldsymbol{I}_{3\times3}$; sampling time $T_s = 0.5$ s. Physical system constraints are: $[10\ 10\ \pi\ 0.65\ 0.5\ 0.8]^{\mathrm{T}} \leq \boldsymbol{x} \leq [10\ 10\ \pi\ -0.5\ 0.5\ 0.8]^{\mathrm{T}}$ and $\boldsymbol{\tau}_{\max} = -\boldsymbol{\tau}_{\min} = [7\ 4\ 4]^{\mathrm{T}}$. Note that the simulated vessel dynamics (1)–(2) are based on a 1:70 small-scaled vessel model, CS II (Fossen, 2011). Therefore, the parameter values involved in the system dynamics and constraints have been down-scaled accordingly based on the Froude scaling law (Moreira et al., 2007). All the algorithms are implemented in MATLAB 2016b (MATLAB, 2016) with solver Cplex (ILOG, 2010) on a platform with Intel(R) Core(TM) i3-7100 CPU @3.70 GHz.

5.1. Full state feedback robust DP

When full system states are measured accurately, the vessel's real trajectory is confined within a tube with a nominal trajectory as the center and an offline computed robust positive invariant set as the cross section. As the nominal trajectory converges to the origin, the tube that contains the real trajectory converges to a bounded neighborhood of the origin. As shown in Fig. 4, the vessel is initially positioned at $(-1, -1)$ with uncertain environmental disturbances. With the proposed robust DP controller, the green nominal trajectory converges to $(0, 0)$. Around the discrete nominal north-east positions, we also plot the robust positive invariant bounded sets $\mathbb{S}$ that form the tube together with the nominal trajectory. The red real trajectory then evolves within the tube and also converges to and maintains at the neighborhood of origin although environmental disturbances exist.

By solving the nominal MPC problem (21), original system constraints are tightened. Fig. 5 and Fig. 6 show the speed and control input trajectories, respectively, on surge, sway and yaw. The nominal

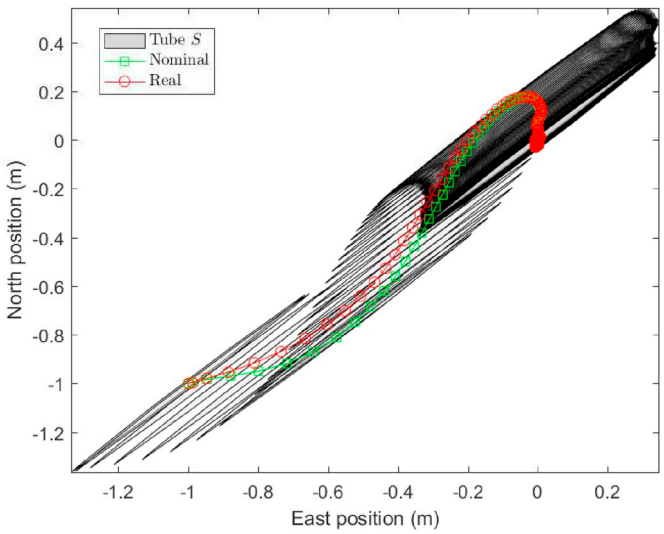

Fig. 4. Trajectories and trajectory tubes with full state feedback.

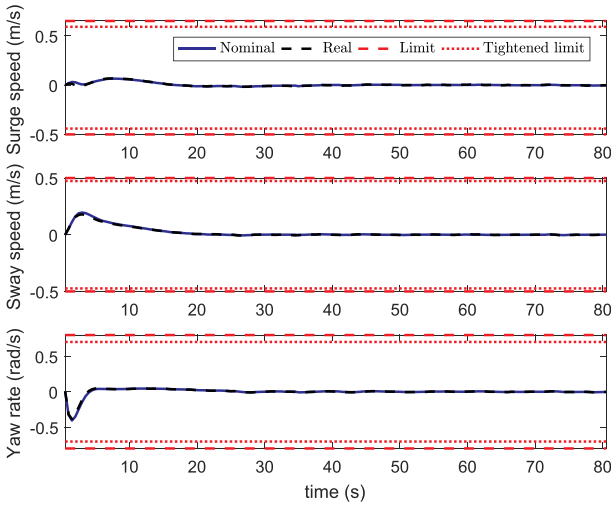

Fig. 5. Speed trajectories with full state feedback.

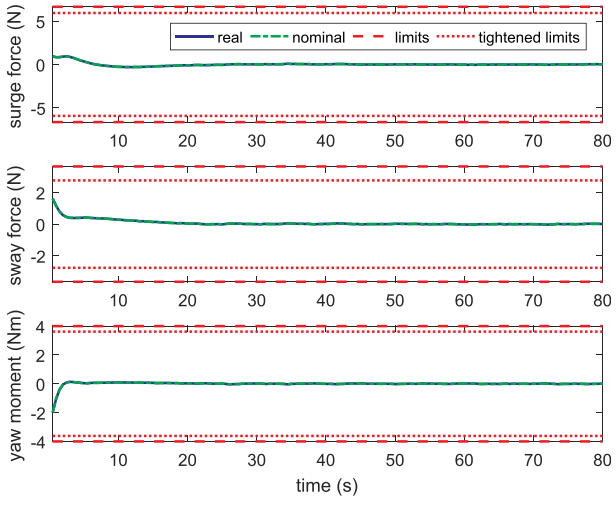

Fig. 6. Input trajectories with full state feedback.

trajectories satisfy the tightened constraints and the real trajectory satisfy the original constraints. Fig. 7 and Fig. 8 further show the constraint satisfactions of the speed and control input trajectory over the prediction horizon at one time step. Note that the nominal and real trajectories are not fitting tightly to the system limits. This is partly due to the design of tube cross-sections, and partly due to the approximated feedback control policy (12) for the trade-off between conservativeness and computational complexity.

5.2. Output feedback robust DP

When only partial system states are measured with errors, Fig. 9 shows the nominal trajectory, the estimated trajectory and the real vessel trajectory from the initial position to the origin. It can be seen that the nominal trajectory converges to and stabilizes at the origin. The estimated and real trajectories converges to and maintains at the corresponding robust invariant sets $\mathbb{S}$ and $\mathbb{S} \oplus \tilde{\mathbb{S}}$ around the origin. To show the tube and the trajectories more clearly, we further plot the three dimensional set series in Fig. 10.

Similar with the full state feedback robust DP controller, system constraints are also all satisfied with the output feedback robust DP controller, as shown in Fig. 11 and Fig. 12 for trajectories over the entire simulation and Fig. 13 and Fig. 14 over the prediction horizon at one time step. The nominal trajectories are restricted within the tightened constraint limits and the real trajectories are restricted within the original constraint limits. The difference between the tightened and original limits can be seen as a type of buffer zones saved for the uncertain bounded disturbances.

5.3. Comparisons of the two robust DP controllers

In practice, whether employing the full state feedback controller or the output feedback controller depends on the availability of precise state measurements. However, to further explore the control performance in simulations, we report the comparison results of the proposed robust controllers. In Fig. 15, the east position and north position trajectories of the two controllers are plotted. The trajectories controlled by both controllers can converge to zero robustly with comparable tracking errors. However, the full state feedback controller has faster convergence speed than the oput feedback controller. This is not doubtful since the full state feedback controller has more accurate dynamic system information in real-time.

To relieve the potential computational burden of the MPC online optimization problems, linearized prediction models (10) are used

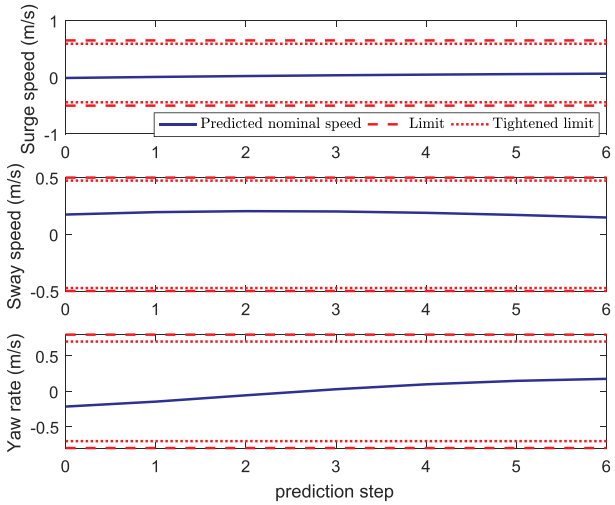

Fig. 7. Predicted speed trajectories with full state feedback.

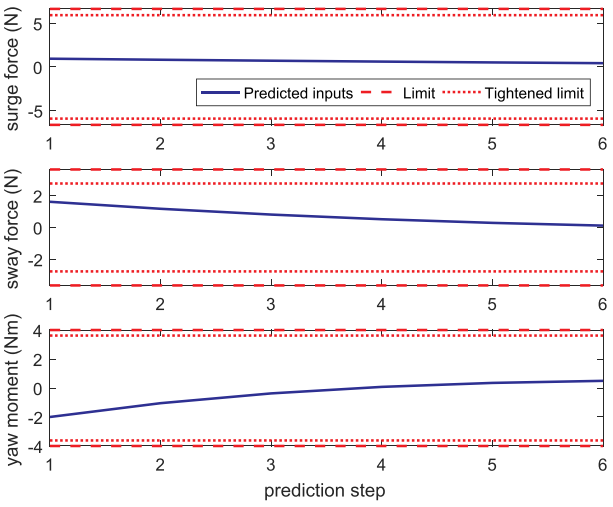

Fig. 8. Predicted input trajectories with full state feedback.

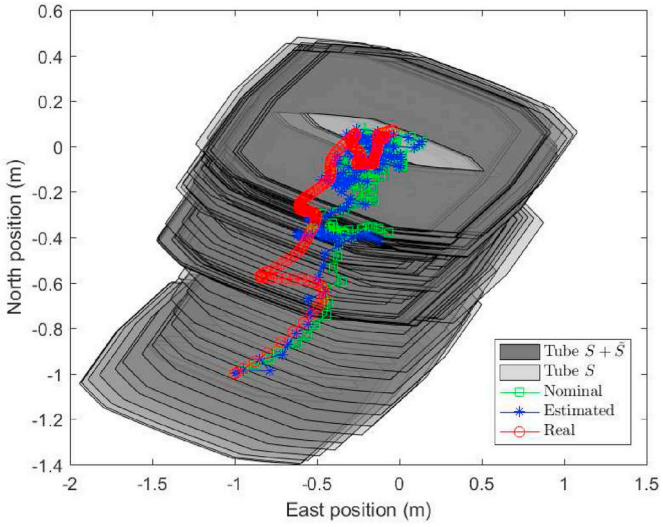

Fig. 9. Trajectories and trajectory tubes with output feedback.

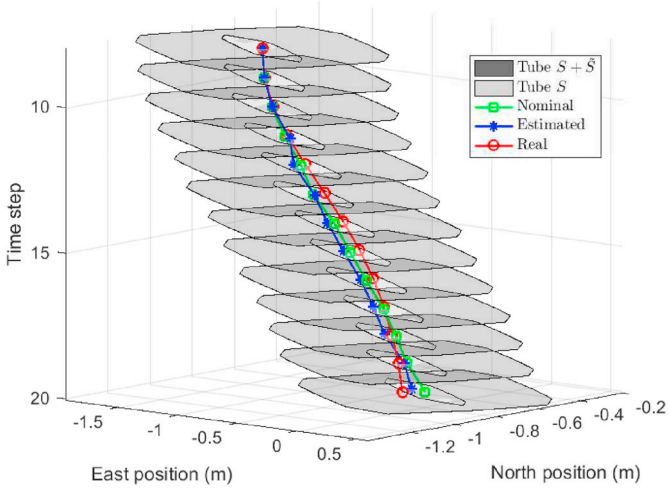

Fig. 10. Trajectories and trajectory tubes with output feedback in 3D.

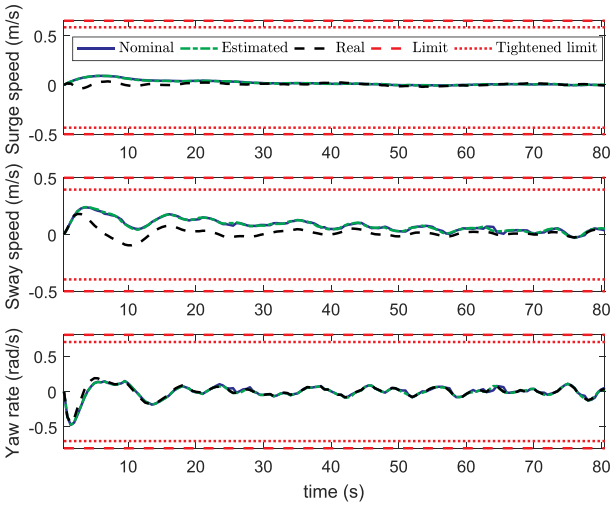

Fig. 11. Speed trajectories with output feedback.

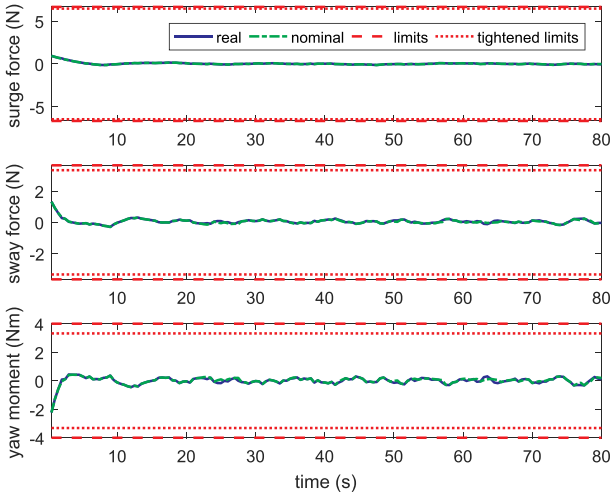

Fig. 12. Input trajectories with output feedback.

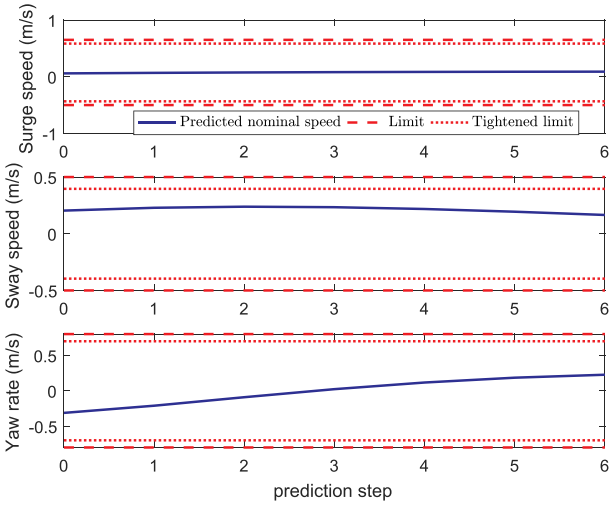

Fig. 13. Predicted speed trajectories with output feedback.

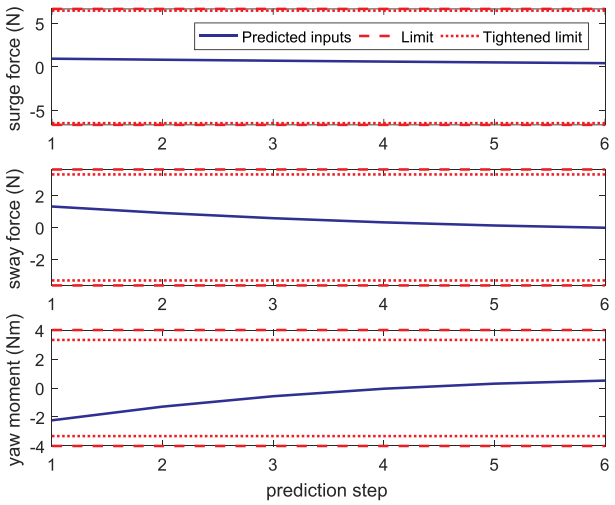

Fig. 14. Predicted input trajectories with output feedback.

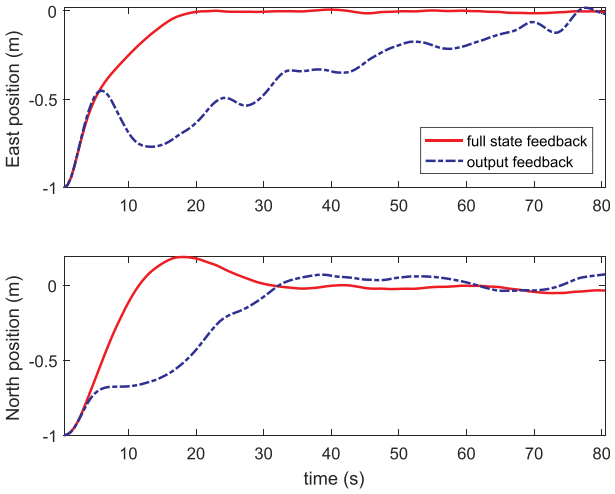

Fig. 15. Comparison on the tracking performance.

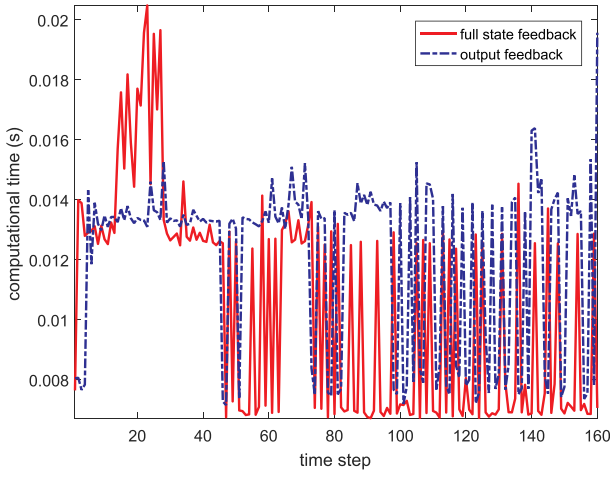

Fig. 16. Comparison on the computational times.

instead of highly nonlinear dynamics (1)–(2). Therefore, the involved online problems are all convex and can be efficiently solved. The computational times of the proposed full state feedback and output feedback robust controllers are reported in Fig. 16. It can be observed that the computational times of the two proposed robust controllers are comparable. Throughout the simulations, the computational times are all around 15 ms and are all far smaller than the system sampling time $T_s = 0.5$. s. It thus can be concluded that the proposed robust dynamics positioning controllers are in principle suitable for real-time applications.

6. Conclusions and future work

Depending on whether accurate full vessel states being available or not, this paper proposes two robust dynamic positioning (DP) approaches for autonomous surface vessels (ASVs). The control goals to guarantee that the vessel's pose converges to and maintains within a bounded neighborhood of the specified DP pose have been well achieved under uncertain environmental disturbances. We have considered high fidelity nonlinear vessel hydrodynamics and used an approximated linear model in the tube-based MPC controller design. All the possible uncertain system trajectories lie in a tube that is guided by a nominal trajectory towards the origin and confined by precomputed robust positive invariant sets. The online optimization problems have comparable complexity with that of conventional MPC. Moreover, a Luenberger observer is designed to estimate the system states when only vessel poses are available with measurement errors. The resultant estimation errors and measurement errors are further incorporated in the tube-based MPC. Simulation results have demonstrated the effectiveness of the proposed robust DP controllers in both full state and output feedback cases. Future research will consider robust trajectory tracking problems of ASVs with environmental disturbances.

CRediT author statement

Huarong Zheng: Conceptualization, Methodology, Software, Writing - Original draft preparation.

Jun Wu: Data curation, Investigation, Supervision.

Weimin Wu: Resources, Investigation, Writing - Reviewing and Editing, Supervision, Funding acquisition.

Yifeng Zhang: Writing -Reviewing and Editing.

Declaration of competing interest

None.

Acknowledgements

This research is supported in part by the China Postdoctoral Science Foundation, China, under Grant 2019M652086, in part by the National Natural Science Foundation of China under Grants 61773343, in part by the Key Research and Development Program of Guangdong Province of China under Grant 2019B010120001, and in part by the Project of State Key Laboratory of Industrial Control Technology (Zhejiang University) of China under Grant ICT1921.

References

Cetin, S., Akkaya, A.V., 2010. Simulation and hybrid fuzzy-PID control for positioning of a hydraulic system. Nonlinear Dynam. 61 (3), 465–476.

Chen, L., Hopman, H., Negenborn, R.R., 2018. Distributed model predictive control for vessel train formations of cooperative multi-vessel systems. Transport. Res. C Emerg. Technol. 92, 101–118.

Du, J., Hu, X., Liu, H., Chen, C.L.P., 2015. Adaptive robust output feedback control for a marine dynamic positioning system based on a high-gain observer. IEEE Trans. Neural Network Learn. Syst. 26 (11), 2775–2786.

Du, J., Xin, H., Krstić, M., Sun, Y., 2016. Robust dynamic positioning of ships with disturbances under input saturation. Automatica 73 (C), 207–214.

Fossen, T.I., 2011. Handbook of Marine Craft Hydrodynamics and Motion Control. John Wiley and Sons Ltd, West Sussex, U.K.

Fossen, T., Perez, T., 2009. Kalman filtering for positioning and heading control of ships and offshore rigs. IEEE Contr. Syst. Mag. 29 (6), 32–46.

Fossen, T.I., Strand, J.P., 1999. Passive nonlinear observer design for ships using lyapunov methods: full-scale experiments with a supply vessel. Automatica 35 (1), 3–16.
Hou, M., Pugh, A.C., Raste, T., Muller, P.C., 1999. On luenberger observer design for constrained mechanical systems. J. Dyn. Syst. Meas. Contr. 121 (2), 322–326.
ILOG, 2010. IBM ILOG CPLEX optimizer [Online]. Available. http://www-01.ibm.com/software/integration/optimization/cplex-optimizer/.
Jia, D., Krogh, B., 2002. Min-max feedback model predictive control for distributed control with communication. In: Proceedings of the 2002 American Control Conference. (ACC), Anchorage, USA, pp. 4507–4512.
Kouvaritakis, B., Cannon, M., Raković, S.V., Cheng, Q., 2010. Explicit use of probabilistic distributions in linear predictive control. Automatica 46 (10), 1719–1724.
Li, H., Yan, W., 2017. Model predictive stabilization of constrained underactuated autonomous underwater vehicles with guaranteed feasibility and stability. IEEE ASME Trans. Mechatron. 22 (3), 1185–1194.
Lin, X., Nie, J., Jiao, Y., Liang, K., Li, H., 2018. Nonlinear adaptive fuzzy output-feedback controller design for dynamic positioning system of ships. Ocean. Eng. 158, 186–195.
MATLAB, R2016b, 2016. Natick. The MathWorks Inc., Massachusetts.
Mayne, D.Q., 2014. Model predictive control: recent developments and future promise. Automatica 50 (12), 2967–2986.
Mayne, D.Q., Rawlings, J.B., Rao, C.V., Scokaert, P.O.M., 2000. Constrained model predictive control: stability and optimality. Automatica 36 (6), 789–814.
Mayne, D.Q., Seron, M.M., Raković, S., 2005. Robust model predictive control of constrained linear systems with bounded disturbances. Automatica 41 (2), 219–224.
Mayne, D.Q., Rakovic, S., Findeisen, R., Allgower, F., 2006. Robust output feedback model predictive control of constrained linear systems. Automatica 42, 1217–1222.
Moreira, L., Fossen, T.I., Soares, C.G., 2007. Path following control system for a tanker ship model. Ocean. Eng. 34 (14), 2074–2085.
Port of Rotterdam, 2015. Expected Weather Conditions in the Port of Rotterdam. https://www.portofrotterdam.com/en/shipping/up-to-date-information/current-water-levels-flow-wind-and-visibility.
Rakovic, S.V., Kerrigan, E., Kouramas, K., Mayne, D., 2005. Invariant approximations of the minimal robust positively invariant set. IEEE Trans. Automat. Contr. 50 (3), 406–410.
Raković, S.V., Kouvaritakis, B., Cannon, M., Panos, C., Findeisen, R., 2012. Parameterized tube model predictive control. IEEE Trans. Automat. Contr. 57 (11), 2746–2761.
Sørensen, A., 2011. A survey of dynamic positioning control systems. Annu. Rev. Contr. 35 (1), 123–136.
Sørensen, A., Sagatun, S., Fossen, T., 1996. Design of a dynamic positioning system using model-based control. Contr. Eng. Pract. 4 (3), 359–368.
Tannuri, E.A., Agostinho, A., Morishita, H., Jr, L.M., 2010. Dynamic positioning systems: an experimental analysis of sliding mode control. Contr. Eng. Pract. 18 (10), 1121–1132.
Torsetnes, G., Jouffroy, J., Fossen, T.I., 2004. Nonlinear dynamic positioning of ships with gain-scheduled wave filtering. In: Proceedings of IEEE Conference on Decision & Control. Nassau, Bahamas, USA, pp. 5340–5347.
Værnø, S.A., Brodtkorb, A.H., Skjetne, R., 2019. Compensation of bias loads in dynamic positioning of marine surface vessels. Ocean. Eng. 178, 484–492. https://doi.org/10.1016/j.oceaneng.2019.03.010.
Veksler, A.V., Johansen, T.A., Borrelli, F., Realfsen, B., 2016. Dynamic positioning with model predictive control. IEEE Trans. Contr. Syst. Technol. 24 (4), 1340–1353.
Witkowska, A., Śmierzchalski, R., 2018. Adaptive dynamic control allocation for dynamic positioning of marine vessel based on backstepping method and sequential quadratic programming. Ocean. Eng. 163, 570–582.
Yan, Z., Wang, J., 2012. Model predictive control for tracking of underactuated vessels based on recurrent neural networks. IEEE J. Ocean. Eng. 37 (4), 717–726.
Zheng, H., Negenborn, R.R., Lodewijks, G., 2013. Survey of approaches for improving the intelligence of marine surface vehicles. In: Proceedings of the 16th International IEEE Conference on Intelligent Transportation Systems, pp. 1217–1223. The Hauge, The Netherlands.
Zheng, H., Negenborn, R.R., Lodewijks, G., 2014. Trajectory tracking of autonomous vessels using model predictive control. In: Proceedings of the 19th IFAC World Congress, pp. 8812–8818. Cape Town, South Africa.
Zheng, H., Negenborn, R.R., Lodewijks, G., 2016a. Explicit use of probabilistic distributions in robust predictive control of waterborne AGVs – a cost-effective approach. In: Proceedings of the 15th European Control Conference. IFAC, Aalborg, Denmark, pp. 1278–1283.
Zheng, H., Negenborn, R.R., Lodewijks, G., 2016b. Predictive path following with arrival time awareness for waterborne AGVs. Transport. Res. C Emerg. Technol. 70, 214–237.
Zheng, H., Negenborn, R.R., Lodewijks, G., 2018. Robust distributed predictive control of waterborne AGVs–a cooperative and cost-effective approach. IEEE Trans. Cybern. 48 (8), 2449–2461.